四川大学学报（医学版） 2026，57（1）：154－159
J Sichuan Univ（Med Sci）

在线全文

糖尿病视网膜病变微血管改变定量评估及其与血视网膜屏障破坏的关联研究*

雷颖庆，吕红彬△，周 琦，田 敏，曹 阳
西南医科大学附属医院 眼科（泸州 646000）

【摘要】 目的 基于光学相干断层扫描血管成像（optical coherence tomography angiography, OCTA）技术定量评估糖尿病视网膜病变（diabetic retinopathy, DR）患者的视网膜微血管改变，并探讨其与血视网膜屏障（blood-retinal barrier, BRB）破坏的关联。**方法** 纳入本院收治的208例2型糖尿病合并DR患者，行OCTA检查获取视网膜微血管参数；同步检测血清血管内皮生长因子（vascular endothelial growth factor, VEGF）和细胞间黏附因子1（intercellular adhesion molecule 1, ICAM-1）水平。分析OCTA参数与血清标志物的相关性，采用Logistic回归分析危险因素，并通过受试者工作特征曲线（receiver operating characteristic curve, ROC）曲线评估诊断效能。**结果** 208例DR患者浅层毛细血管密度（superficial capillary density, SCP-D）和深层毛细血管密度（deep capillary density, DCP-D）分别为（42.67±4.35）%、（47.89±5.02）%；中心凹无血管区（foveal avascular zone, FAZ）面积、周长、圆形指数均值分别为（0.38±0.10）mm^2、（2.04±0.28）mm、0.72±0.08；无灌注区面积均值（1.87±0.45）mm^2。其中121例（58.17%）SCP-D异常（<45%），114例（56.25%）DCP-D异常（<50%），88例（42.31%）FAZ面积异常，77例（37.02%）FAZ周长异常，69例（33.17%）FAZ圆形指数异常；142例（68.27%）无灌注区面积异常。FAZ面积与VEGF〔r=0.559，95%置信区间（confidence interval, CI）：0.457～0.661〕、ICAM-1（r=0.411，95%CI：0.289～0.533）呈正相关；FAZ圆形指数、SCP-D、DCP-D与VEGF及ICAM-1均呈负相关（P<0.05）；无灌注区面积与二者呈正相关。Logistic回归显示，糖尿病病程〔比值比（odds ratio, OR）=1.159，95%CI：1.060～1.267〕及VEGF（OR=1.013，95%CI：1.005～1.022）是发生严重视网膜微血管改变的独立危险因素（P<0.05）。4个OCTA评估指标中无灌注区面积的预测价值最高，曲线下面积（area under the curve, AUC）为0.879（95%CI：0.820～0.938）。**结论** DR患者的OCTA评估指标水平与BRB相关标志物密切相关，无灌注区面积对于DR患者发生严重视网膜微血管改变的预测价值最高。

【关键词】 糖尿病视网膜病变 光学相干断层扫描血管成像 视网膜微血管改变 血视网膜屏障

Quantitative Assessment of Microvascular Changes in Diabetic Retinopathy and Their Association With Blood-Retinal Barrier Impairment

LEI Yingqing, LÜ Hongbin△, ZHOU Qi, TIAN Min, CAO Yang. Ophthalmology Department, The Affiliated Hospital of Southwest Medical University, Luzhou 646000, China
△ Corresponding author, E-mail: oculistlvhongbin1@163.com

This study was supported by the 2024 Central Guided Local Science and Technology Development Fund Project of Sichuan Provincial Science and Technology Department (No. 2024ZYD0114) and the Medical Science and Technology Project of Sichuan Medical Association (No. 202407100226).

[Abstract] Objective To quantitatively evaluate retinal microvascular changes in patients with diabetic retinopathy (DR) using optical coherence tomography angiography (OCTA), and to explore their association with blood-retinal barrier (BRB) disruption. **Methods** A total of 208 patients with type 2 diabetes and DR underwent OCTA to obtain microvascular parameters. Serum vascular endothelial growth factor (VEGF) and intercellular adhesion molecule 1 (ICAM-1) levels were measured. Correlations were analyzed, risk factors were identified using logistic regression, and diagnostic efficacy was evaluated with ROC curves. **Results** The superficial capillary density (SCP-D) and deep capillary density (DCP-D) of the 208 DR patients were (42.67 ± 4.35)% and (47.89 ± 5.02)%, respectively. The mean values for the area, perimeter, and circularity index of the foveal avascular zone (FAZ) were (0.38 ± 0.10) mm^2, (2.04 ± 0.28) mm, and 0.72 ± 0.08, respectively. The mean area of the non-perfusion zone was (1.87 ± 0.45) mm^2. Among these patients, 121 (58.17%) cases had abnormal SCP-D (< 45%), 114 (56.25%) cases had abnormal DCP-D (< 50%), 88 (42.31%) cases had abnormal FAZ area, 77 (37.02%) cases had abnormal FAZ perimeter, 69 (33.17%) cases had abnormal FAZ circularity

* 四川省科学技术厅2024年中央引导地方科技发展基金（No. 2024ZYD0114）和四川省医学会医学科技项目（No. 202407100226）资助
△ 通信作者，E-mail: oculistlvhongbin1@163.com
出版日期：2026-01-20

index, and 142 (68.27%) cases had abnormal non-perfusion zone area. The FAZ area was positively correlated with VEGF (r = 0.559, 95% CI: 0.457-0.661) and ICAM-1 (r = 0.411, 95% CI: 0.289-0.533). The FAZ circularity index, SCP-D, and DCP-D were negatively correlated with VEGF and ICAM-1 (P < 0.05). The area of the non-perfusion zone was positively correlated with both. Logistic regression showed that the duration of diabetes (odds ratio [OR] = 1.159, 95% CI: 1.060-1.267) and VEGF (OR = 1.013, 95% CI: 1.005-1.022) were independent risk factors for severe retinal microvascular changes (P < 0.05). Among the four OCTA assessment indicators, the area of the non-perfusion zone had the highest predictive value, with an area under the curve (AUC) of 0.879 (95% CI: 0.820-0.938). **Conclusion** The OCTA assessment indicators in DR patients are closely related to BRB-related markers. The area of the non-perfusion zone has the highest predictive value for severe retinal microvascular changes in DR patients.

[Key words] Diabetic retinopathy　Optical coherence tomography angiography　Retinal microvascular alterations　Blood-retinal barrier

糖尿病视网膜病变(diabetic retinopathy, DR)是糖尿病患者常见微血管并发症及主要致盲原因[1]。其发病机制复杂, 早期以微血管异常为主, 其中血视网膜屏障(blood-retinal barrier, BRB)功能破坏和周细胞丢失被认为是关键环节[2]。可直接导致毛细血管瘤形成、内皮细胞增殖失控及视网膜渗漏和无灌注区域扩展加剧[3-4]。光学相干断层扫描血管成像(optical coherence tomography angiography, OCTA)作为一种无创、高分辨率血管成像技术, 为DR早期评估[4]及微循环障碍机制研究提供了新的可视化与定量手段[5-6]。然而, 目前关于OCTA如何定量反映周细胞丢失及其与BRB破坏程度之间的关联研究仍不充分[7]。为此, 本研究利用OCTA获取并分析DR患者的微血管图像的, 结合生物标志物与BRB通透性指标, 探讨OCTA微血管参数与血清中BRB相关标志物血管内皮生长因子(vascular endothelial growth factor, VEGF)和细胞间黏附分子-1(intercellular adhesion molecule 1, ICAM-1)水平之间的关联性。旨在阐明DR早期血管病变机制, 为开发精准化、个体化的DR诊疗策略提供理论依据与影像学支撑。

1　资料与方法

1.1　一般资料

本研究为回顾性临床研究, 纳入对象为2022年1月–2024年6月期间在本院就诊的DR患者, 患者均已签署知情同意书, 本研究经西南医科大学附属医院伦理委员会批准(批号: S2024001)。纳入标准: ①符合世界卫生组织(WHO)2019年糖尿病诊断标准, 确诊为2型糖尿病; ②经眼底检查或OCTA确诊为非增殖期DR(NPDR)或增殖期DR(PDR); ③糖尿病病程≥5年; ④过去3个月内测定过HbA1c水平, 并记录完整; ⑤能配合完成OCTA成像, 图像质量评分≥7分(标准评分范围0 ~ 10); ⑥单眼受累或双眼受累但仅选取单眼图像进行分析。排除标准如下: ①合并其他视网膜疾病, 如老年性黄斑变性、视网膜静脉阻塞、视网膜色素变性等(共排除18例); ②既往有视网膜激光治疗、玻璃体手术史者(排除23例); ③有明显屈光间质混浊, 如严重白内障或玻璃体混浊, 影响OCTA图像质量者(排除12例); ④合并系统性严重疾病(如恶性肿瘤、肝肾功能衰竭)或精神类疾病(排除6例); ⑤妊娠期糖尿病患者(排除3例)。最终纳入208例患者。

1.2　方法

1.2.1　基线资料收集

①一般资料: 收集患者年龄、性别、糖尿病病程、体质量指数(body mass index, BMI)、收缩压(systolic pressure, SBP)及舒张压(diastolic pressure, DBP)。②糖尿病控制情况: 采集近3个月内糖化血红蛋白(glycated hemoglobin, HbA1c)与空腹血糖(fasting blood glucose, FPG)值。③眼科检查指标: 测量眼轴长度、最小分辨角对数视力(logMAR BCVA)及眼压。所有数据录入数据库并进行质量控制, 确保可重复性。

1.2.2　检测方法

(1)OCTA图像采集与分析: 采用AngioVue OCTA系统对患者散瞳后视网膜进行3 mm×3 mm和6 mm×6 mm扫描。图像信号强度指数需≥7, 由两名评估者盲法判读, 不一致时由第三位专家裁定。依据国际分层共识, 使用内置软件分析浅层毛细血管密度(superficial capillary density, SCP-D)、深层毛细血管密度(deep capillary density, DCP-D)、中心凹无血管区(foveal avascular zone, FAZ)面积、周长、圆形指数及无灌注区面积, 各指标判定异常标准[8]为: SCP-D<45%, DCP-D<50%, FAZ面积>0.40 mm^2, FAZ圆形指数<0.75, 无灌注区面积>1.5 mm^2。本研究将满足以下至少两项者定义为“严重视网膜微血管改变”: ①SCP-D<43.5%; ②DCP-D< 45.1%; ③FAZ面积>0.4 mm^2; ④无灌注区面积>1.65 mm^2。(2)血清生化指标检测: 采集患者清晨空腹静脉血, 离心分离血清, −80 ℃保存。使用R&D公司ELISA试剂盒, 严格按说明书操作检测血清VEGF和ICAM-1水平。

1.3 统计学方法

采用SPSS 26.0软件进行数据分析。计量资料以$\bar{x}\pm s$表示，计数资料以频数和百分比表示。采用Pearson或Spearman相关性分析探讨OCTA参数与血清标志物的关联。采用多因素logistic回归分析周细胞丢失的独立危险因素，结果以比值比(odds ratio, OR)及其95%置信区间(confidence interval, CI)表示。采用受试者工作特征曲线评估OCTA参数的诊断效能，并计算曲线下面积(area under the curve, AUC)及其95%CI。所有统计学检验均采用双侧检验，P<0.05为差异有统计学意义。

2 结果

2.1 患者基线资料情况

208例研究对象的平均年龄为(57.23±8.19)岁；男性 113 例，占比 54.33%，女性 95 例，占比 45.67%；糖尿病病程平均为(9.12±3.41)年。基线资料方面，BMI为(24.88±3.15) kg/m^2；SBP为(129.42±13.82) mmHg (1 mmHg=0.133 kPa)，DBP为(80.09±9.06) mmHg。血糖相关指标显示，HbA1c均值为(7.86±1.32)%，FPG为(8.47±1.89) mmol/L。眼部相关检测指标结果为：眼轴长度平均(23.52±0.85) mm；logMAR BCVA均值0.38±0.17；眼压平均水平(15.71±2.83) mmHg。

2.2 OCTA图像指标情况

208例DR患者SCP-D和DCP-D分别为(42.67±4.35)%、(47.89±5.02)%，121例(58.17%)SCP-D异常，114例(56.25%)DCP-D异常；黄斑无血管区面积、周长、圆形指数均值(0.38±0.10) mm^2、(2.04±0.28) mm、0.72±0.08，异常率42.31%(88例)、37.02%(77例)以及33.17%(69例)；无灌注区面积均值(1.87±0.45) mm^2，142例(68.27%)异常(图1)。

2.3 血清生化指标情况

208例DR患者的VEGF为(267.53±45.21) pg/mL，其中89例(42.79%)患者VEGF异常；ICAM-1为(312.47±58.37) ng/mL，其中65例(31.25%)患者ICAM-1异常。

2.4 OCTA微血管参数与血清BRB相关标志物相关性分析

FAZ面积与VEGF和ICAM-1水平均呈正相关，SCP-D、DCP-D与、FAZ圆形指其呈负相关，差异有统计学意义(表1)。

2.5 影响严重视网膜微血管改变的多因素logistic回归分析结果

本组患者性别比、BMI等基线资料都在正常参考值范围内，故未纳入多因素logistic回归分析模型。经分析，发现患者的糖尿病病程(OR=1.159，P=0.001)和VEGF水平(OR=1.013，P<0.001)是发生严重视网膜微血管改变的独立危险因素(表2)。

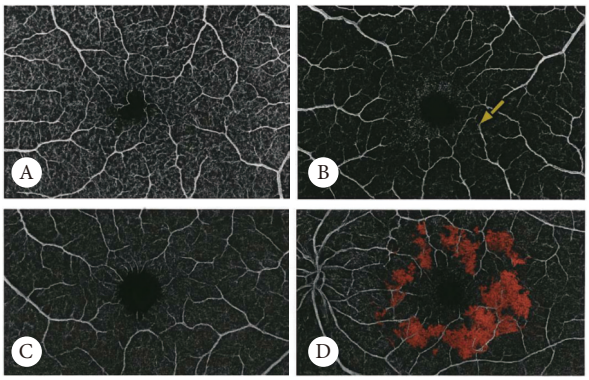

图 1 典型病例OCTA图像

Fig 1 OCTA image of a typical case

A, The 3 mm × 3 mm scan revealed diffuse hypoperfusion of the superficial capillary plexus (SCP-D = 41%) and a sparse, fragmented vascular grid. B, The 3 mm × 3 mm scan showed a significant reduction in the density of the deep capillary plexus (DCP-D = 46%), accompanied by microaneurysms (yellow arrow). C, The 3 mm × 3 mm scan indicated that the area of the FAZ analysis diagram expanded (0.42 mm^2) and its shape was irregular (circular index [CI] = 0.68). D, The 6 mm × 6 mm scan revealed extensive areas of non-perfusion (marked in red, with an area of 1.92 mm^2), and the area of pericyte loss overlapped significantly with the area of barrier disruption. Image quality: SSI = 8/10, double blind verification.

表 1 OCTA微血管参数与血清BRB相关标志物相关性分析结果(r)

Table 1 Correlation analysis results between OCTA microvascular parameters and serum BRB-related markers (r)

OCTA parameter	VEGF	ICAM-1
FAZ area	0.559*	0.411**
FAZ circularity index	−0.392**	−0.425**
SCP-D	−0.512**	−0.466**
DCP-D	−0.447**	−0.379**
Non-perfusion area	0.559**	0.411**

FAZ: foveal avascular zone; SCP-D: superficial capillary density; DCP-D: deep capillary density. n=208. * P < 0.05, ** P < 0.01.

2.6 OCTA参数对严重视网膜微血管改变的诊断效能

以“重度微血管改变”作为金标准，即真阳性标准。单独使用DCP-D、SCP-D、FAZ面积及无灌注区面积作为诊断指标均对基于OCTA定义的严重视网膜微血管改变具有良好诊断价值，其中无灌注区面积AUC最高(0.879，95%CI: 0.820 ~ 0.938)，敏感度85.06%，特异度78.75%，约登指数最大(0.6375)(表3、图2)。

3 讨论

本研究以OCTA为核心技术平台，结合血清生物标

表 2　Logistics回归分析结果

Table 2　Logistic regression analysis results

Variable	β	SE	Wald χ^2	P	OR	95% CI
Age	0.023	0.017	1.829	0.176	1.023	0.990-1.057
Diabetes duration	0.148	0.046	10.361	0.001	1.159	1.060-1.267
Axial length	0.015	0.009	2.778	0.186	1.015	0.992-1.039
HbA1c	0.108	0.091	1.406	0.236	1.114	0.933-1.330
VEGF	0.013	0.004	11.077	< 0.001	1.013	1.005-1.022
ICAM-1	0.005	0.003	2.329	0.127	1.005	0.998-1.013
IL-6	0.009	0.007	1.709	0.191	1.009	0.996-1.023
Constant	−4.216	1.534	7.549	0.006	—	—

HbA1c: glycated hemoglobin; VEGF: vascular endothelial growth factor; ICAM-1: intercellular adhesion molecule 1; IL-6: interleukin 6; β: partial regression coefficient; SE: standard error; OR: odds ratio.

表 3　OCTA参数对严重视网膜微血管改变的诊断效能分析结果

Table 3　Diagnostic performance of OCTA parameters for severe retinal microvascular alterations

Parameter	Cut-off value	Sensitivity	Specificity	AUC	95% CI	Youden index
DCP-D	45.1%	83.12%	76.25	0.873	0.812 – 0.933	0.593 7
SCP-D	43.5%	78.57%	72.5	0.842	0.775 – 0.909	0.511 0
FAZ area	0.4 mm²	70.13%	80	0.826	0.754 – 0.897	0.501 3
Non-perfusion area	1.65 mm²	85.06%	78.75	0.879	0.820 – 0.938	0.637 5

DCP-D: deep capillary density; SCP-D: superficial capillary density; FAZ: foveal avascular zone; AUC: area under the curve.

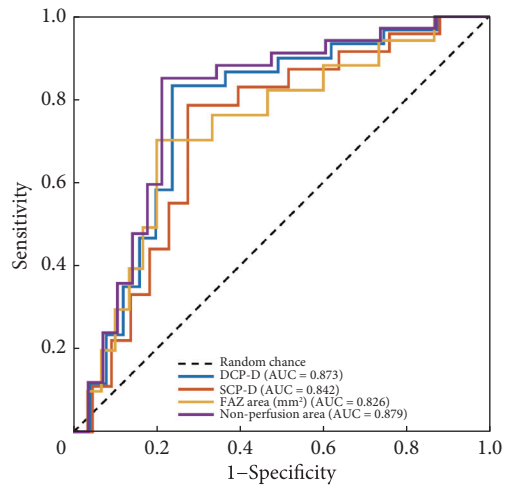

图 2 OCTA参数对严重视网膜微血管改变的诊断效能ROC曲线

Fig 2 ROC curve of diagnostic efficacy of OCTA parameters for severe retinal microvascular changes

志物检测，分析了糖尿病视网膜病变（DR）患者视网膜微血管参数改变与血清中血视网膜屏障（BRB）相关标志物水平之间的关联性。研究结果显示，随着DR分期的进展，视网膜浅层（SCP）和深层（DCP）毛细血管密度显著降低，FAZ面积扩大，形态趋于不规则，非灌注区面积增大。同时，血清VEGF和ICAM-1水平均呈显著升高趋势。这些发现共同提示OCTA所观测的微血管结构异常与系统性及潜在眼部的血管炎症、内皮功能障碍（反映在血清VEGF、ICAM-1升高）存在显著关联，间接支持了周细胞丢失与BRB破坏在DR进展中的关键作用。FAZ面积扩大与圆形指数下降进一步强化了这一判断。本研究中糖尿病相关眼部血管指标（SCP-D、DCP-D 等）及血清VEGF、ICAM-1 水平异常率显著，相较于以往研究报道的健康人群[9-11]，本研究 FAZ 面积增大、血管密度降低，结合血清炎症及血管生成因子升高，提示这些指标或可作为糖尿病视网膜病变早期筛查的潜在生物标志物。FAZ作为无血管区，对视网膜中心区的供血需求高度敏感，其面积扩大和边缘不规则正是毛细血管闭塞的结果[12]。有研究显示FAZ圆形指数下降与毛细血管的环状排列紊乱密切相关，而这种排列紊乱正是因周细胞凋亡、毛细血管网断裂、血流重新分布所致[13]。

非灌注区域面积的扩大也为周细胞凋亡提供了佐证[14]。无灌注区是视网膜毛细血管闭塞后形成的区域，与视网膜缺血密切相关[15]。本研究显示无灌注区面积与VEGF、ICAM-1浓度呈显著正相关，说明随着微血管功能的逐步丧失，视网膜组织产生缺血信号，引发VEGF等因子的过度表达。VEGF作为血管通透性调节的关键分子，

其升高直接导致BRB完整性破坏，使血浆成分外渗、视网膜水肿形成[16]。ICAM-1则介导白细胞黏附与内皮激活，进一步加剧局部炎症与血管壁损伤[17]。ROC结果提示浅层毛细血管的灌注状态同样具有一定的预测能力。FAZ面积与无灌注区面积的AUC值尽管略低于深层密度指标，但仍具备一定的诊断价值，符合既往关于“深层毛细血管丛是DR早期微血管病变靶点”的研究理论[18-19]。

研究发现，周细胞通过α-平滑肌肌动蛋白(α-SMA)及PDGFR-β信号维持毛细血管的收缩和支撑能力，一旦周细胞脱落，毛细血管易发生结构失稳，导致局部管腔狭窄、断裂，最终形成灌注缺血灶[20]。视网膜微血管改变引发内皮细胞紧密连接松解，从而导致BRB功能障碍[21]。VEGF通过与VEGFR-2结合激活PI3K/Akt通路，增加血管通透性；ICAM-1激活NF-κB通路，引导免疫细胞向局部聚集，共同促进渗漏和水肿的发生[22-23]。与以往研究主要依赖动物模型或组织切片不同，本研究验证了视网膜微血管改变与BRB破坏之间的强关联性[24]。目前OCTA技术尚无法在体直接观察和定量单个周细胞，本研究中对周细胞丢失的探讨是基于其已知的、会导致特定微血管改变(如毛细血管失稳、退化、闭塞)的理论基础，通过分析这些可观测的OCTA参数来实现的间接评估。未来研究可扩大样本规模，开展多中心、纵向随访研究，结合更多血清标志物与OCTA参数，构建多维预测模型，进一步明确其在早期诊断和干预中的应用价值。

综上，本研究以OCTA技术为依托，系统揭示了糖尿病视网膜病变中周细胞丢失与血视网膜屏障破坏之间的密切联系，提出了以毛细血管密度、FAZ结构和无灌注区面积为核心的量化评估指标，并通过与血清VEGF、ICAM-1水平的耦合分析，构建了“结构—功能—分子”三重证据链条，为理解DR早期病变机制和制定精准诊疗策略提供了基础。

* * *

作者贡献声明 雷颖庆负责论文构思、正式分析、经费获取、研究方法、初稿写作和审读与编辑写作，吕红彬负责数据审编、研究项目管理、提供资源和监督指导，周琦负责调查研究，田敏负责验证和可视化，曹阳负责软件。所有作者已经同意将文章提交给本刊，且对将要发表的版本进行最终定稿，并同意对工作的所有方面负责。

Author Contribution LEI Yingqing is responsible for conceptualization, formal analysis, funding acquisition, methodology, writing--original draft, and writing--review and editing. LÜ Hongbin is responsible for data curation, project administration, resources, and supervision. ZHOU Qi is responsible for investigation. TIAN Min is responsible for validation and visualization. CAO Yang is responsible for software. All authors consented to the submission of the article to the Journal. All authors approved the final version to be published and agreed to take responsibility for all aspects of the work.

利益冲突 所有作者均声明不存在利益冲突

Declaration of Conflicting Interests All authors declare no competing interests.

参 考 文 献

[1] 孙丹丹, 许迅. 褪黑激素对糖尿病视网膜病变内皮细胞及周细胞的保护作用研究现状与进展. 中华眼底病杂志, 2020, 36(9): 745-748. doi: 10.3760/cma.j.cn511434-20190321-00106.
SUN D D, XU X. Research status and progress on the protective effects of melatonin on endothelial cells and pericytes in diabetic retinopathy. Chinese Journal of Ocular Fundus Diseases, 2020, 36(9): 745-748. doi: 10.3760/cma.j.cn511434-20190321-00106.

[2] 雷林旖, 曹原, 姚进. 小胶质细胞参与的细胞间通讯在视网膜神经血管单元中的作用. 中华实验眼科杂志, 2024, 42(11): 1060-1064. doi: 10.3760/cma.j.cn115989-20230627-00025.
LEI L Y, CAO Y, YAO J. Role of microglia-mediated intercellular communication in the retinal neurovascular unit. Chinese Journal of Experimental Ophthalmology, 2024, 42(11): 1060-1064. doi: 10.3760/cma.j.cn115989-20230627-00025.

[3] 周婧, 韩梅. 非奈利酮通过抑制小胶质细胞炎症反应减轻大鼠糖尿病视网膜病变. 中国病理生理杂志, 2023, 39(8): 1483-1490. doi: 10.3969/j.issn.1000-4718.2023.08.017.
ZHOU J, HAN M. Finerenone alleviates diabetic retinopathy in rats by inhibiting microglial inflammatory response. Chinese Journal of Pathophysiology, 2023, 39(8): 1483-1490. doi: 10.3969/j.issn.1000-4718.2023.08.017.

[4] 钟缘, 蒋鹏飞, 赵盼, 等. 基于PI3K/AKT信号通路探讨益气养阴活血利水方抑制早期糖尿病视网膜病变大鼠微血管周细胞凋亡的作用机制. 湖南中医药大学学报, 2023, 43(11): 2024-2033. doi: 10.3969/j.issn.1674-070X.2023.11.015.
ZHONG Y, JIANG P F, ZHAO P, *et al*. Mechanism of Yiqi Yangyin Huoxue Lishui Recipe in inhibiting microvascular pericyte apoptosis in early diabetic retinopathy rats based on PI3K/AKT signaling pathway. Journal of Hunan University of Chinese Medicine, 2023, 43(11): 2024-2033. doi: 10.3969/j.issn.1674-070X.2023.11.015.

[5] 龚珂, 唐莉, 孙文涛等. 人血管内皮抑素对糖尿病大鼠视网膜病变的干预效果及对VCAM-1, ICAM-1以及VEGF等蛋白表达的影响. 临床和实验医学杂志, 2021, 20(11): 1143-1147. doi: 10.3969/j.issn.1671-4695.2021.11.007.
GONG K, TANG L, SUN W T, *et al*. Intervention effect of human endostatin on diabetic retinopathy in rats and its influence on the expression of VCAM-1, ICAM-1, and VEGF proteins. Journal of Clinical and Experimental Medicine, 2021, 20(11): 1143-1147. doi: 10.3969/j.issn.1671-4695.2021.11.007.

[6] DHARMARAJAN S, CARRILLO C, QI Z, *et al*. Retinal inflammation in murine models of type 1 and type 2 diabetes with diabetic retinopathy. Diabetologia, 2023, 66(11): 2170-2185. doi: 10.1007/s00125-023-05995-4.

[7] YUN J H. Hepatocyte growth factor prevents pericyte loss in diabetic retinopathy. Microvasc Res, 2021, 133: 104103. doi: 10.1016/j.mvr.2020.104103.

[8] XU S, GAO F, LUAN R, *et al*. Normative data and correlation parameters for vessel density measured by 6×6-mm optical coherence tomography angiography in a large Chinese urban healthy elderly population: data from the Beichen eye study. BMC Ophthalmol, 2024, 24: 298. doi: 10.1186/s12886-024-03561-z.

[9] GUPTA P, THAKAR M, RAJURKAR K, *et al*. Analysis of foveal avascular zone by using spectral-domain optical coherence tomography angiography in healthy Indian eyes. Indian J Ophthalmol, 2024, 72(6): 838-843. doi: 10.4103/IJO.IJO_2212_23.

[10] O'SHEA S M, O'DWYER V M, SCANLON G. Normative data on the foveal avascular zone in a young healthy Irish population using optical coherence tomography angiography. Eur J Ophthalmol, 2022, 32(5): 2824-2832. doi: 10.1177/11206721211073446.

[11] ALDAKHIL S, CHALLA N, ALHOSHAN S A, *et al*. Quantitative analysis

of early retinal changes and OCT parameters in diabetic subjects with and without retinopathy. Diagnostics (Basel), 2025, 15(4): 451. doi: 10.3390/diagnostics15040451.

[12] YUN J H. Interleukin-1β induces pericyte apoptosis via the NF-κB pathway in diabetic retinopathy. Biochem Biophys Res Commun, 2021, 546: 46-53. doi: 10.1016/j.bbrc.2021.01.108.

[13] HUANG B B, FUKUYAMA H, BURNS S A, *et al*. Imaging the retinal vascular mural cells *in vivo*: Elucidating the timeline of their loss in diabetic retinopathy. Arterioscler Thromb Vasc Biol, 2024, 44(2): 465-476. doi: 10.1161/ATVBAHA.

[14] HERDADE A S, SILVA I M, CALADO Â, *et al*. Effects of diabetes on microcirculation and leukostasis in retinal and non-ocular tissues: Implications for diabetic retinopathy. Biomolecules, 2020, 10(11): 1583. doi: 10.3390/biom10111583.

[15] NING J, PAN M, YANG H, *et al*. Melatonin attenuates diabetic retinopathy by regulating EndMT of retinal vascular endothelial cells via inhibiting the HDAC7/FOXO1/ZEB1 axis. J Pineal Res, 2024, 76(6): e13008. doi: 10.1111/jpi.13008.

[16] WANG Y, YANG X, LI Q, *et al*. Single-cell RNA sequencing reveals the Müller subtypes and inner blood-retinal barrier regulatory network in early diabetic retinopathy. Front Mol Neurosci, 2022, 15: 1048634. doi: 10.3389/fnmol.2022.1048634.

[17] RANGASAMY S, MONICKARAJ F, LEGENDRE C, *et al*. Transcriptomics analysis of pericytes from retinas of diabetic animals reveals novel genes and molecular pathways relevant to blood-retinal barrier alterations in diabetic retinopathy. Exp Eye Res, 2020, 195: 108043. doi: 10.1016/j.exer.2020.108043.

[18] SIVAPRASAD Sφφ, SEN S, CUNHA-VAZ J. Perspectives of diabetic retinopathy-challenges and opportunities. Eye (Lond), 2023, 37(11): 2183-2191. doi: 10.1038/s41433-022-02335-5.

[19] HUANG Z, CHU W K, NG T K, *et al*. Protective effects of nattokinase against microvasculopathy and neuroinflammation in diabetic retinopathy. J Diabetes, 2023, 15(10): 866-880. doi: 10.1111/1753-0407.13439.

[20] ELEFTHERIOU C G, IVANOVA E, SAGDULLAEV B T. Of neurons and pericytes: The neuro-vascular approach to diabetic retinopathy. Vis Neurosci, 2020, 37: E005. doi: 10.1017/S0952523820000048.

[21] FRESTA C G, FIDILIO A, CARUSO G, *et al*. A new human blood-retinal barrier model based on endothelial cells, pericytes, and astrocytes. Int J Mol Sci, 2020, 21(5): 1636. doi: 10.3390/ijms21051636.

[22] MONICKARAJ F, ACOSTA G, CABRERA A P, *et al*. Transcriptomic profiling reveals chemokine CXCL1 as a mediator for neutrophil recruitment associated with blood-retinal barrier alteration in diabetic retinopathy. Diabetes, 2023, 72(6): 781-794. doi: 10.2337/db22-0619.

[23] PARK W, KIM J, CHOI S, *et al*. Human plasminogen-derived N-acetyl-Arg-Leu-Tyr-Glu antagonizes VEGFR-2 to prevent blood-retinal barrier breakdown in diabetic mice. Biomed Pharmacother, 2021, 134: 111110. doi: 10.1016/j.biopha.2020.111110.

[24] SHENG X, ZHANG C, ZHAO J, *et al*. Microvascular destabilization and intricated network of the cytokines in diabetic retinopathy: from the perspective of cellular and molecular components. Cell Biosci, 2024, 14(1): 85. doi: 10.1186/s13578-024-01269-7.

（2025 – 06 – 06收稿, 2025 – 12 – 18修回）

编辑　汤　洁